



Effect of soil pH on the transport, fractionation, and oxidation of chromium (III)

Teng Xu^a, Feng Nan^b, Xiaofeng Jiang^a, Yuling Tang^b, Yunhang Zeng^b, Wenhua Zhang^{a,b,*}, Bi Shi^a

^a Key Laboratory of Leather Chemistry and Engineering of Ministry of Education, Sichuan University, Chengdu, 610065, China

^b National Engineering Laboratory for Clean Technology of Leather Manufacture, Sichuan University, Chengdu, 610065, China

ARTICLE INFO

Keywords:

Trivalent chromium
Hexavalent chromium
Soil pH
FTIR
XPS

ABSTRACT

This work was conducted to study the effect of soil pH (4.0, 6.0, and 8.0) on the transport, fractionation, and oxidation of trivalent chromium [Cr(III)]. Variation in pH altered soil chemical and mineralogical properties such as zeta potential, cation exchange capacity and redox potential of natural soil. Breakthrough curves and batch sorption experiments coupled with fourier transform infrared spectroscopy (FTIR) and X-ray photoelectron spectroscopy (XPS) analyses demonstrated that the easy mobility of Cr(III) in pH 4.0 soil was dominated by the limited coordination effect. The high retention of Cr(III) in pH 8.0 soil was mainly ascribed to the hydrolysis. Incubation experiments indicated that the proportions of Cr in exchangeable fraction decreased with increasing of soil pH and incubation time, and kinetics analysis revealed that the time dependent transformation was controlled by mass transfer and chemical processes (e.g., hydrolysis, ion association). The XPS confirmed the oxidation of Cr(III) in pH 8.0 soil during the incubation period. Furthermore, the content of toxic hexavalent chromium [Cr(VI)] was positively associated with time and initial concentration of Cr(III) released. These results revealed the hazardousness of Cr(III) in soil contaminated simultaneously by inorganic acid and alkali.

1. Introduction

Soil contamination by anthropogenic chromium (Cr) is a worldwide problem (Shahid et al., 2017). Several industrial activities such as leather tanning, wood preservation and metal finishing are the main sources of Cr pollution (Choppala et al., 2018; Farid et al., 2018). In the leather industry, large amounts of Cr-containing effluents, shavings, and sludge are produced due to the common use of basic chromium sulfate (Zhang et al., 2017). Environmental seepage may occur through multiple pathways, such as inadvertent dripping of Cr tanning liquor (containing Cr 3000 mg L⁻¹) (Zhou et al., 2012), leaking of tannery wastewater (up to 1500 mg L⁻¹) (Religa et al., 2011), and poor storage or indiscriminate dumping and landfill of sludge (up to 40,000 mg kg⁻¹) (Alibardi and Cossu, 2016). The released Cr would eventually enter soil, and the spatial distribution of Cr and site pH are closely related to leather production. Only Cr(III) is used in the leather industry, which is considered to be less toxic and mobile than Cr(VI). Cr (III) is the main contaminant in the soil of tannery sites, but Cr(VI) has also been detected. Soil within the vicinity of the tannery wastewater discharge site in the Sialkot of Pakistan has total Cr of 21–675 mg kg⁻¹ and pH of 7.1–10.6 (Ali et al., 2015). Soil in a tannery room in

California (USA) has total Cr of 130–22,000 mg kg⁻¹, Cr(VI) of 1 < to 187 mg kg⁻¹, and pH of 4.6–7.8 (Makdisi, 1991). These site investigations reveal that soil in tannery sites is contaminated simultaneously by Cr(III) and inorganic acid and alkali, such as sulfuric acid in the pickling and sodium hydroxide in the soaking during leather manufacture (Covington, 2009). Assessment of the environmental risk of Cr in soil is of utmost importance and depends on thorough understanding of the transport, solid-phase fractionation, and oxidation behavior of Cr(III) in soils with different pH levels.

The vertical distribution of Cr(III) in soils can be strongly localized by transport limitations, and laboratory column experiments of Cr-containing liquid flowing through soil media are commonly designed to simulate Cr transport and retention (Banks et al., 2006; Zhang et al., 2018b). Scholars have extensively investigated factors influencing Cr transport and retention particularly for cases involving soil structure, soil minerals, organic matter, microbial exopolymeric substances, and flow rate (Akhtar et al., 2011; Hu et al., 2010; Jardine et al., 1999; Kantar et al., 2011). However, information about the effect of soil pH on the behavior of Cr(III) transport is lacking.

The geochemical fractionation of Cr is crucial in understanding the mobility and bioavailability of Cr in soils (Ertani et al., 2017), among

* Corresponding author. The Key Laboratory of Leather Chemistry and Engineering of Ministry of Education, SICHUAN University, No.24 South Section 1, Yihuan Road, Chengdu, 610065, China.

E-mail address: zhangwh@scu.edu.cn (W. Zhang).

<https://doi.org/10.1016/j.ecoenv.2020.110459>

Received 19 December 2019; Received in revised form 25 February 2020; Accepted 7 March 2020

Available online 14 March 2020

0147-6513/© 2020 The Authors. Published by Elsevier Inc. This is an open access article under the CC BY-NC-ND license

(<http://creativecommons.org/licenses/by-nc-nd/4.0/>).

which the exchangeable Cr is considered to be the most easily mobile and bioavailable fraction using sequential extraction method (Tessier et al., 1979). Aceves et al. (2007) found the exchangeable Cr in tannery sludge-amended soil decreased with prolonged incubation time. However, Taghipour and Jalali (2015) reported the exchangeable Cr in soil with 5% leather factory waste increased from 7.4 to 201.6 mg kg⁻¹ when incubation lasting from 15 to 90 days. Different phenomena suggest that the factors affecting the fractionation of Cr in soil are complicated, and previous studies have mainly focused on applying substances to affect the fractionation of Cr. Various amendments, such as citric acid, polyaspartic acid, soil organic, and zerovalent iron, affect fractionation by mobilization or immobilization of Cr in soil (Balasoiu et al., 2001; Fu et al., 2017; Li et al., 2017; Su et al., 2016). Nevertheless, limited studies have focused on the effect of soil pH on the fractionation of Cr.

The conversion of Cr(III) into Cr(VI) is undesirable and hazardous from an environmental perspective because Cr(VI) is a known carcinogen (Hausladen and Fendorf, 2017). The oxidation of Cr(III) to Cr(VI) was highly concerned and extensively studied in solution system. However, the behavior of metal in homogenous system is very different from that in heterogenous system especially in media of soil. The effects of pH on the fate of Cr(III) in soil was mainly centered on the oxidation according to existing literature, and studied by using soil/water suspension to simulate the behavior of Cr in soil. For example, Bartlett and James (1979) devised a suspension system containing 1:2000 of super-soil-to-solution of CrCl₃ to study the effects of pH on Cr(III) oxidation by adjusting liquid phase pH from 3.0 to 10.0. They found lower pH facilitated the formation of Cr(VI), and at pH 3.2 all Cr(III) was oxidized to Cr(VI). Reijonen and Hartikainen (2016) used soils incubated at pH 4.4, 5.5 and 6.2 to study the oxidation of CrCl₃ solution in suspension system with soil/solution ratio of 1:10, and no Cr(VI) was found in soil without addition of MnO₂. Obviously, these studies were very different from the real environment which was conducted in semi-arid soil. Hence, the effect of pH on the oxidation of Cr(III) in semi-arid soil requires systematic study.

In this study, we investigated the soil pH-dependent mechanisms of the transport, fractionation, and oxidation of Cr(III) to reveal the risk of the release of Cr(III) from tannery sites. Experiments on soil column were carried out to obtain the retention characteristics of Cr(III), and the results were quantified and compared using sorption isotherms. Incubation experiments were performed to determine the behavior underlying the transformation of Cr into various fractions and the oxidation of Cr(III) into Cr(VI) in semi-arid soils. The kinetics of transformation and oxidation of Cr(III) were also investigated in soil with three pH levels.

2. Materials and methods

2.1. Materials

2.1.1. Chemicals

All chemicals including magnesium chloride (MgCl₂), sodium acetate (NaOAc), hydroxylamine hydrochloride (NH₂OH·HCl), acetic acid (HOAc), nitric acid (HNO₃), ammonium acetate (NH₄OAc), sulfuric acid (H₂SO₄), sodium hydroxide (NaOH), basic chromium sulfate [Cr(OH)SO₄], sodium chloride (NaCl), sodium bromide (NaBr), and diphenylcarbazide were analytical reagent grade, and purchased from Aladdin (Shanghai, China). Milli-Q water was used for the preparation of samples and standard solutions.

2.1.2. Soil

The test soil used in the experiment was collected from the topsoil (0–20 cm) of bare arable land in eastern China (37°22'N 118°02'E), homogenized, air dried, crushed, and sieved (stainless steel sieve, Ø 2 mm). Sieved soil was stored at 4 °C until use as natural soil. The results of the content of each substance in the soil were expressed on a

dry weight basis by oven drying (3 g of soil at 105 °C for ~ 15 h).

The soils used for column experiment were divided into three groups and chemically adjusted to pH 4.0 ± 0.1, 6.0 ± 0.1, and 8.0 ± 0.1, respectively, which represented a range of soil pHs according to the actual investigation results at tannery pollution sites (Ali et al., 2015; Makdisi, 1991). Soil pH was lowered by addition of H₂SO₄ solution (1 mol L⁻¹) and elevated by NaOH solution (0.5 mol L⁻¹) to obtain target pHs. H₂SO₄ and NaOH were used to adjust soil pH (Obia et al., 2015) for their common use in pickling, soaking, and liming during leather manufacture (Covington, 2009; Font et al., 1998). Soil pH was continuously adjusted for two weeks to ensure pH stability and air dried before use. The pre-adjusted pH soil samples amended with Cr(OH)SO₄, which was widely used in tannery (Panda et al., 2016), were used for incubation experiment and maintained at target pH values by periodically addition of H₂SO₄ or NaOH solution.

2.2. Design of the experiments

2.2.1. Column transport and batch sorption experiments

Transport of Cr(III) solutions was examined with a plexiglass column (12 cm long, 1.6-cm i. d.) packed with pH-preadjusted soil samples without addition of Cr(III). 23.2 g air-dried soil sample was packed in the column with approximately 8 cm height. The column was fitted with quartz sand (2-cm thick layer) and nylon sieve (50-µm pore size) at the bottom and top to reduce soil deformation and soil colloid release caused by solution infiltration. The column was preconditioned by pumping 5 mmol L⁻¹ NaCl solution in the upward direction. The flow rate was set as 1 mL min⁻¹ and controlled by a calibrated peristaltic pump (silicone tubing). A total of at least 50 pore volumes were eluted during conditioning. The equilibration period ensured that water flow and ionic strength in the soil column remained stable during the experiments. After soil colloid stabilization, the feed solution was replaced with 3000 mg L⁻¹ (57.69 mmol L⁻¹) Cr(III) [as Cr(OH)SO₄]. The concentration was selected considering the typical Cr content in Cr tanning liquor (Zhou et al., 2012) and was higher than the limit of 1.5 mg L⁻¹ defined by the Chinese Environmental Protection Agency (GB 30486–2013). Following injection, column effluent was collected at intervals of 3 min by using an automatic collector to analyze Cr content. Br⁻ (0.75 mmol L⁻¹) of NaBr was injected as a tracer to confirm the closely identical hydrodynamic properties of each packed soil column (Calderer et al., 2014). The pore volume was estimated to be approximately 0.3 mL by using the methods of Kantar et al. (2011). The diagram of the soil column experimental device is shown in Supplementary Fig. S1, and the parameters of the soil column are listed in Table S1.

Two different sets of sorption experiments were conducted to understand the mechanisms of Cr(III) retention in soil columns. The first set of experiments aimed at understanding the general sorption equilibrium and the effect of soil pH on sorption capacity. In the second set of experiments, the contact time of the Cr-soil suspension was varied from 1 min to 24 h to test the sorption kinetics of Cr(III) in soils of different pH levels. The experimental procedures are detailed in supplementary data section 2.

2.2.2. Incubation

Incubation experiment was used to study the fractionation and oxidation of Cr in soil at three pH levels. Cr(III) was added to soil at 600 mg kg⁻¹. The dose was selected as a criterion near the value of typical Cr content in tannery site (Ali et al., 2015) and was higher than the limit of 350 mg kg⁻¹ defined by the Chinese Environmental Protection Agency (GB 15618–2018). The incubation soil samples retained water content equivalent to 15% of the soil weight by periodic addition of distilled water. The soil samples were incubated for up to 150 days at 303 K and the soils were collected for determination of total Cr content in each fraction and Cr(VI) content at certain time intervals.

2.3. Analytical methods

Soil properties including soil texture, soil pH, cation exchange capacity (CEC), organic matter (OM), redox potential (Eh), Cr(VI), and soil digestion were analyzed using Chinese standard methods. The standard method numbers are listed in [Supplementary Table S2](#). Cr(VI) was extracted from the soil samples by using the method of [Bartlett and James \(1979\)](#), as described in detail in supplementary data (section 4). The extracts were then analyzed by spectrophotometric colorimetric method.

Metal elemental analyses were performed by inductively coupled plasma optical emission spectroscopy (ICP-OES, OPTIMA 8000DV, PerkinElmer, USA), $\lambda_{Cr} = 267.7/283.5$ nm, $\lambda_{Fe} = 238.2/259.9$ nm and $\lambda_{Mn} = 257.6/259.3$ nm. Total carbon, inorganic carbon (IC) and total nitrogen (TN) in soils were determined by using a carbon and nitrogen analyzer (Primacs100, Skalar, Netherlands). Zeta potential of the soil samples was measured by an autotitrator and zeta potential analyzer (NanoBrook Omni, Brookhaven, USA). The concentration of tracer bromide ion (Br^-) in the column effluent was determined by ion chromatography (ICS-600, Thermo Fisher, USA) with IonPac CS12A column (4 × 250 mm) and 30 mmol L⁻¹ KOH as the mobile phase at a flow rate of 1 mL min⁻¹. The main mineral of the natural soil was determined by X-ray diffractometer (XRD, DX-2000, Aolong, China). The XRD patterns of natural soil and mineral components in natural soil are shown in supplementary data ([Fig. S2](#) and [Table S3](#)). The properties of soil sample before and after pH adjustment are listed in [Table 1](#).

The sequential extraction method (supplementary data, [Table S4](#)) was used to classify and quantify individual Cr fraction ([Tessier et al., 1979](#)). Fourier transform infrared spectroscopy (FTIR, IS10, Thermo Fisher Scientific, USA) was used to characterize functional group changes in the soil samples after pH adjustment and Cr(III) treatment. Surface elemental analysis of natural and Cr(III)-amended soils was conducted by X-ray photoelectron spectroscopy (XPS, XSAM800, Kratos, UK). The soil with an initial Cr(III) content of 5000 mg kg⁻¹ and after 90 days of incubation was used for XPS analyses because XPS spectra cannot display characteristic peaks if Cr content was low ([Boursiquot et al., 2002](#)).

2.4. Data analysis

2.4.1. Retardation factor

The retardation factor (R) of three soil types was determined from the breakthrough curves according to the following equation ([Godoy et al., 2019](#)):

$$R = \frac{PV_i}{PV} \quad (1)$$

where PV_i is the corresponding pore volume number when outflow concentration (C) of Cr(III) reaches half of the initial concentration (C_0), i.e., $C/C_0 = 0.5$, and PV is the corresponding pore volume number when the tracer bromide ion outflow concentration $C/C_0 = 0.5$.

Table 1

Properties of soil sample before and after pH adjustment.

pH(H ₂ O)	Eh ^a	CEC ^a	OM ^a	IC ^a	OC ^a	TN ^a	Cr	Fe	Mn	Soil texture
	mV	cmol ⁺ kg ⁻¹	g kg ⁻¹							
8.64 (natural)	476	6.79	7.96	10.26	3.22	1.21	0.041	23.11	0.42	C _{6.20} I _{29.73} A _{64.07} ^b
8.0 ± 0.1	491	6.71	7.83	9.32	3.09	0.46	0.047	24.09	0.41	C _{6.05} I _{28.45} A _{65.50}
6.0 ± 0.1	540	5.97	7.37	1.94	2.85	0.55	0.038	24.92	0.45	C _{10.48} I _{27.71} A _{61.81}
4.0 ± 0.1	557	5.36	7.72	0.19	2.89	0.76	0.045	22.15	0.41	C _{4.26} I _{23.67} A _{72.07}

^a Eh, redox potential; CEC, cation exchange capacity; OM, organic matter; IC, inorganic carbon; OC, inorganic carbon; TN, total nitrogen.

^b Numerical subscripts refer to weight percentage of each texture in natural soil. C, clay; I, silt; A, sand. According to international soil texture classification, the soil used in this experiment is sandy loam. All soil properties were measured after two weeks of incubation.

2.4.2. Mobility index (MI)

The mobility of Cr could be associated with the amount of exchangeable Cr in the soil, which could be calculated according to the equation as following ([Taghipour and Jalali, 2015](#)):

$$MI = \sum_{i=1}^n \frac{C_{e_i}/q_i}{n} \quad (2)$$

where C_e is the Cr concentration in exchangeable fraction (mg kg⁻¹), T is the total concentration of the Cr (mg kg⁻¹), and n is the number of the soil samples.

2.4.3. Kinetic models

(1) Diffusion kinetics model

In order to analyze the transformation process of exchangeable Cr, diffusion kinetics model was applied to fit the transformation kinetics data. The decreases of Cr in exchangeable forms could be simulated in a linear relationship with time as the following equation ([Lu et al., 2005](#)):

$$\ln C_e = A + Bt \quad (3)$$

where t is the contact time (day), A and B are the constant of diffusion equation.

(2) Reaction kinetics-based models

The pseudo second-order kinetic model was used to fit the sorption data. The pseudo second-order kinetics model is given as ([Sun et al., 2011](#)):

$$\frac{t}{q_t} = \frac{1}{k_2 q_e^2} + \frac{t}{q_e} \quad (4)$$

where q_e and q_t are the sorption capacity (mmol kg⁻¹) of Cr(III) at equilibrium and at time t (h), respectively, and k_2 [kg (mmol h)⁻¹] is the pseudo second-order rate constant.

The Elovich, first-order and second-order kinetic models have been widely used to describe the kinetics of soil chemical processes, in the present experiment, these models were applied to fit the transformation of exchangeable Cr ([Sparks, 2003](#)). These equations can be expressed as:

Elovich model:

$$q_t = \frac{1}{\beta} \ln \alpha \beta + \frac{1}{\beta} \ln t \quad (5)$$

First order model:

$$\log q_t = \log q_0 - \frac{k_1 t}{2.303} \quad (6)$$

Second order model:

$$\frac{1}{q_t} = \frac{1}{q_0} + k_2 t \quad (7)$$

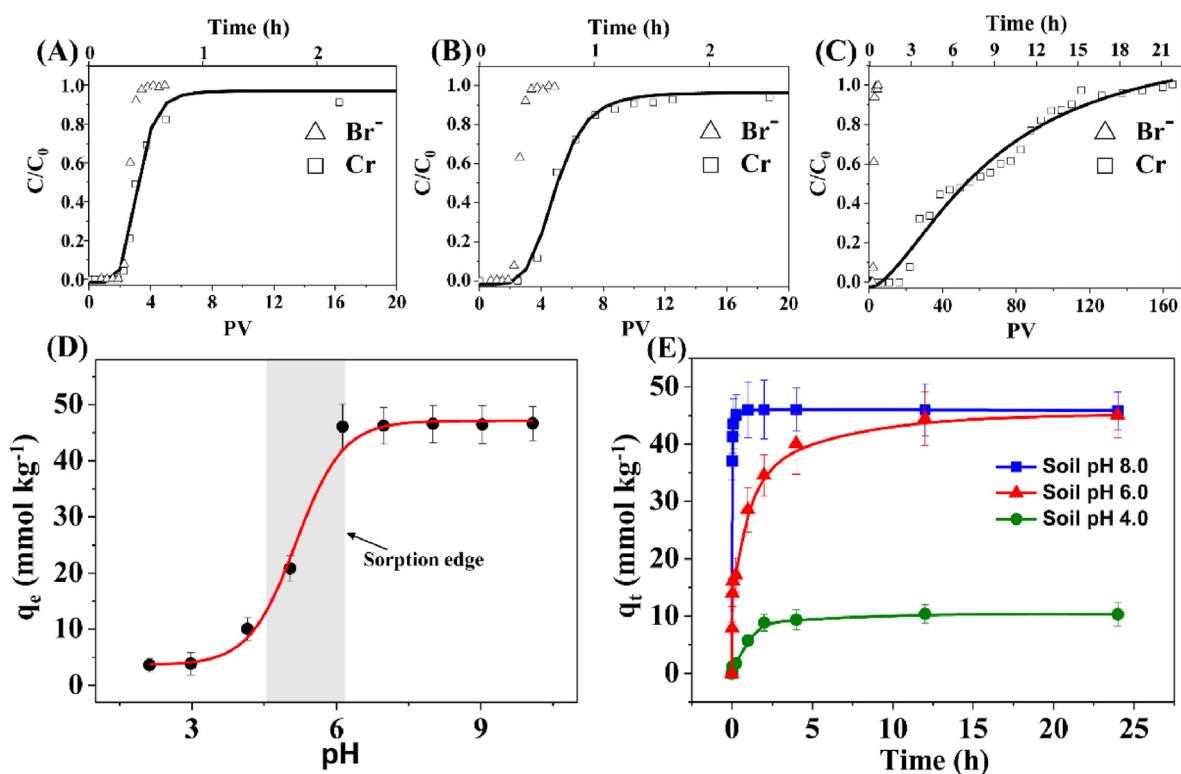


Fig. 1. Breakthrough curves of Cr(III) in various pH soils column: (A) soil pH 4.0; (B) soil pH 6.0; (C) soil pH 8.0. (D) Cr(III) sorption on soil sample as a function of pH. (E) Kinetics of Cr(III) sorption on soils with three pH levels. Points represent the experimental data. Continuous lines represent the fitting data.

where q_t and q_0 (mg kg^{-1}) are the amounts of Cr in the exchangeable fraction per unit mass of soil at time t (day) and initial time, respectively; α and β are constants during the experiment; k_1 (day^{-1}) is the constant in first-order model; and k_2 ($\text{kg mg}^{-1} \text{day}^{-1}$) is the constant in second-order model. The first-order kinetic model was also used to describe the oxidation kinetics of Cr(III). Then the q_t and q_0 (mg kg^{-1}) are the amount of Cr(III) per unit mass of soil at time t (day) and initial time, respectively, k_1 (day^{-1}) is the apparent reaction rate constant. Cr(III) content was determined by subtracting Cr(VI) from the total Cr content.

3. Results and discussion

3.1. Transport of Cr(III) in soils at three pH levels

Fig. 1A–C shows the breakthrough curves of tracer Br^- as NaBr and Cr(III) as $\text{Cr}(\text{OH})\text{SO}_4$ in the soil columns at pH 4.0, 6.0 and 8.0, respectively. The breakthrough curves of Br^- were similar in the three soil types. However, the migration of Cr(III) was weakened compared with Br^- and delayed with increasing soil pH. Approximately 3.01 PV was necessary to reach $C/C_0 = 0.5$ for pH 4.0 soil, 4.85 PV for pH 6.0 soil, and 54.21 PV for pH 8.0 soil, indicating significant Cr(III) retention in the column with pH 8.0 soil.

According to Eq. (1), the retardation factors (R) were 1.18, 1.90, and 21.26, for soils with pH of 4.0, 6.0, and 8.0, respectively. A high value of R suggested low transport, indicating that Cr(III) was more mobile in acidic soil than in alkaline soil, consistent with the previous survey (Makdisi, 1991). The breakthrough curves also indicated that the pollution range should easily expand when Cr(III) solution entered acidic soil, whereas large amounts of Cr(III) were retained in alkaline soil. This result may be ascribed to the difference in pH-dependent surface characteristics of soils (e.g., cationic exchange capacity and zeta potential) and the precipitation of Cr(III) as $\text{Cr}(\text{OH})_3$ at high pH.

The soil CEC value signified the capacity to retain cation in a form

that is difficult to leach from soil, which was determined to be 5.36, 5.97, and 6.71 cmol^+/kg for soils with pH 4.0, 6.0, and 8.0, respectively. The higher CEC value of soil showed stronger retention for soluble cationic Cr(III) in soil columns. Meanwhile the point of zero charge of the soil surface was determined as 2.48 (Supplementary Fig. S3), indicating the soil surface charged negatively at the three pH levels. The electrostatic attraction of soil with cationic Cr(III) species also resulted in the retention of Cr(III) in soil columns. In theory, the main species of soluble inorganic Cr(III) varied from mononuclear Cr ions, such as free Cr^{3+} , CrOH^{2+} , and CrSO_4^+ , to polynuclear Cr ions with more positive charges (e.g., $\text{Cr}_2(\text{OH})_2^{4+}$ and $\text{Cr}_3(\text{OH})_4^{5+}$), and the precipitation $\text{Cr}(\text{OH})_3$ became eventually dominant according to Visual MINTEQ ver. 3.0 (Löv et al., 2017) with increasing pH (Supplementary Fig. S4 and Table S5). The electrostatic attraction and cation exchange of soil with soluble cationic Cr(III) species contributed part of the retention of Cr(III) in soil columns with increasing pH. Indeed, precipitation would occur at pH 4.4 with the initial Cr(III) of 57.69 mmol L^{-1} in soil column experiments based on the solubility product constant of $\text{Cr}(\text{OH})_3$ ($k_{\text{sp}} = 6.3 \times 10^{-31}$) (Dean, 1999). Then a large amount of Cr(III) would be retained as immobile precipitate in soil with pH 6.0 and 8.0 because of the ion product beyond k_{sp} , resulting in delay of breakthrough curves. The characteristics of soils at the three pH levels and the precipitation process would constitute the mechanism of transport, which could be further elucidated by sorption process of Cr(III) in soil with various pH levels.

3.2. Sorption of Cr(III) in soils at three pH levels

Sorption experiments can intuitively explain the migration of Cr(III) in soil columns with different pH levels. Sorption capacity of Cr(III) showed a positive correlation with soil pH (Fig. 1D). The capacity was characterized by a sorption edge (Sparks, 2003), which significantly increased from 3.6 mmol kg^{-1} to approximate 46.6 mmol kg^{-1} within a narrow pH range (about 2 units). The sorption started at around pH

4.0 (Fig. 1D). In theory, precipitation would occur at pH 4.8 for initial Cr(III) concentration of 1.92 mmol L^{-1} in the batch sorption experiments, suggesting that sorption was mainly triggered by the adsorption (chemical complexation) (Flogeac et al., 2005) (confirmed further by FTIR results, section 3.5), electrostatic attraction, cation exchange rather than hydrolysis at pH 4.0. A small amount of Cr(III) was fixed in acidic soils due to the limited quantity of functional groups on the soil surface to coordinate, low cation exchange capacity and weak electrostatic attraction. With increasing soil pH, the sorption of Cr(III) on soil mainly involved hydrolysis, which play a key role in the sharp increase in the sorption edge. Hydrolysis equilibrium would shift toward Cr(OH)₃, leading to more Cr(III) was precipitated on the soil with high pH values. The batch sorption experiments illustrated that alkaline soils had higher affinity for Cr(III) than acidic soil, thereby confirming the high retention of Cr(III) in alkaline soil column.

Fig. 1E shows the sorption kinetics of Cr(III) on soils at the three pH levels. The sorption of Cr(III) by pH 8.0 soil almost reached equilibrium within 5 min, whereas by soil with pH 4.0 which needed more than 4 h. On account of the slow formation of complex, the findings further speculated that adsorption (chemical complexation) should be the main transport mechanism of Cr(III) at pH 4.0 (Gustafsson et al., 2014; Zhou et al., 2019). With increasing soil pH, the quick sorption equilibrium involved the fast formation of precipitate, because when the ion product far exceeded K_{sp} , the supersaturated solution is extremely unstable and has to precipitate to lower the concentrations (Brady et al., 1990). The hydrolysis of Cr(III) could be the main factor for the fast sorption on alkaline soil and thus led to the transport of Cr(III) was limited in the alkaline soil column due to the dominant deposition of Cr(OH)₃ precipitate on the soil. The sorption kinetics can be well fitted by the pseudo second-order kinetic equation, and the fitting parameters are listed in Table S6 (supplementary data).

3.3. Transformation of Cr fraction in Cr(III)-amended soils at three various pH

Soils amended by 600 mg kg^{-1} Cr(III) were incubated from 1 day to 150 days at the three pH levels. The effects of soil pH and incubation time on the percentage of Cr fraction are shown in Fig. 2A, and the contents of Cr in each fraction are listed in Supplementary Table S7. In natural soils with three pH levels (Fig. 2B), Cr was associated mainly with residual (RS) fraction ($> 68.4\%$) and very low exchangeable (EX) fraction ($< 1.8\%$) in the following order: RS $>$ OX (fraction bound to Fe–Mn oxides) $>$ OM (fraction bound to organic matter) $>$ CB (fraction bound to carbonates) $>$ EX. However, the release of Cr significantly changed the fractionation of Cr in the three soil types, and soil pH had considerable influence on the fraction distribution at the early stage of incubation. For example, the proportion of EX Cr was 66.1% for pH 4.0 soil, 10.1% for pH 6.0 soil, and 2.4% for pH 8.0 soil just after addition of Cr(III) (control). With the extension of incubation time, the percentage of EX and CB Cr fractions decreased significantly over time, and the OX fraction increased evidently. Meanwhile, RS and OM fractions varied slightly during the 150-day incubation in the three soil types. After incubation for 150 days, OX Cr became the predominant fraction in all Cr(III)-amended soils and reached as high as 75.4% in pH 4.0 soil, 78.8% in pH 6.0 soil, and 81.1% in pH 8.0 soil. The percentage of EX Cr reduced to 2.5%, 0.35%, and 0.29% in soils with pH 4.0, 6.0, and 8.0, respectively. These findings could be attributed to the transformation of Cr from loosely bound fractions to strongly bound fractions during incubation and consistent with the practical survey of the contaminated site (Castillo et al., 2012). Therefore, transformation of Cr fraction was spontaneous and proceeded once Cr(III) was released into soil. In addition, no significant increase in RS Cr fraction indicated that the amended Cr was unlikely to enter the crystalline lattice during the incubation period.

The mobility of Cr in soils can be evaluated by the mobility index (MI), which can be calculated from the exchangeable fraction (Eq. (2)).

Exchangeable fraction was considered to be the most mobile and bioavailable portion and the most important form of Cr that could cause environmental risks (Ertani et al., 2017). The high MI values of Cr in soils indicated high environmental risk. At the beginning of incubation, the MI values were 0.66 for pH 4.0 soil, 0.10 for pH 6.0 soil, and 0.024 for pH 8.0 soil (Fig. 2C). MI values generally decreased over time in the three soil types. At the end of the incubation (150 days), the MI values were reduced to 0.025 (pH 4.0), 0.0035 (pH 6.0), and 0.0029 (pH 8.0), respectively. Moreover, the value of MI was generally in the order of pH 4.0 $>$ pH 6.0 $>$ pH 8.0 soil during the entire incubation period, consistent with the order of the retardation factor. Hence, soil acidification would spread the pollution range and enhance bioavailability of Cr(III), thereby posing high risks to the environment, particularly at the early stage of Cr(III) pollution.

In order to further study the transformation of EX Cr with incubation time. Transformation kinetics of Cr in exchangeable fraction into other stable forms were fitted to the linearized diffusion-based kinetic model and reaction kinetics-based empirical models such as first-order equation, second-order equation, and Elovich model to explore the time-dependent process. The calculated parameters are given in Table 2. The values of correlation coefficient (R^2) for the diffusion kinetic model were high (> 0.9342), indicating that the reduction of EX Cr was partly attributed to the diffusive process through the macropores and micropores of the soil. The absolute values of the transformation rate constant B were in the order of pH 6.0 soil $>$ pH 4.0 soil $>$ pH 8.0 soil, indicating easier diffusion of EX Cr in acid soils than in alkaline soils.

The reaction kinetics-based empirical models also well described the rate data based on correlation coefficients. The values of R^2 indicated that the Elovich equation was the best fit for pH 4.0 soil (0.9973), the first-order equation for pH 6.0 soil (0.9645), and the second-order equation for pH 8.0 soil (0.9967). The suitability of a particular kinetic model to each pH was due to the fact that the study was conducted before the transformation equilibrium. The difference in the most appropriate model for soils at the three pH levels indicated various reaction-controlled steps during the transformation of exchangeable Cr. The good fit of the diffusion and reaction models indicated that exchangeable Cr mass transfer and chemical transformation occurred simultaneously and these were difficult to separate.

3.4. Oxidation of Cr in Cr(III)-amended soils

The oxidation of Cr(III) in soil would result in hazardous Cr(VI), which is considered more mobile and toxic than the former. Cr(VI) content was measured from 1 day to 90 days to study Cr(III) oxidation in the soils at the three pH levels. Cr(VI) was undetectable in all soil samples after 1 day of incubation, however significantly increased in pH 8.0 soil with prolonged incubation time. Meanwhile, no Cr(VI) was detected in soils with pH 4.0 and 6.0 soil during the experimental period. After 90 days of application (Fig. 3A), the concentration of Cr(VI) in pH 8.0 soil increased to 5.74 mg kg^{-1} , which was higher than the limitation of Chinese Soil Environmental Quality ($< 3.0 \text{ mg kg}^{-1}$, GB 36600–2018) in spite of the oxidation ratio of Cr(III) only as low as 0.96%. Therefore, the release of Cr(III) into alkaline soil would pose environmental risks with prolonged incubation time.

The behavior of Cr(III) and Cr(VI) in environment is closely depended on pH and Eh of the soil. Fig. 3B displays the Eh measurements in soils at the three pH levels amended with Cr(III). As shown in Fig. 3B, the Eh values of soils with pH 4.0, 6.0, and 8.0 were typically within the ranges of 540–556 mV, 529–539 mV and 480–491 mV, respectively. A significant shift to high potentials occurred with decreasing soil pH. These results were likely to be explained by the equation proposed by Patrick et al. (Sparks, 2003):

$$Eh = E^0 - \frac{59}{n} \log \frac{(Red)}{(Ox)} - 59 \frac{m}{n} pH \quad (8)$$

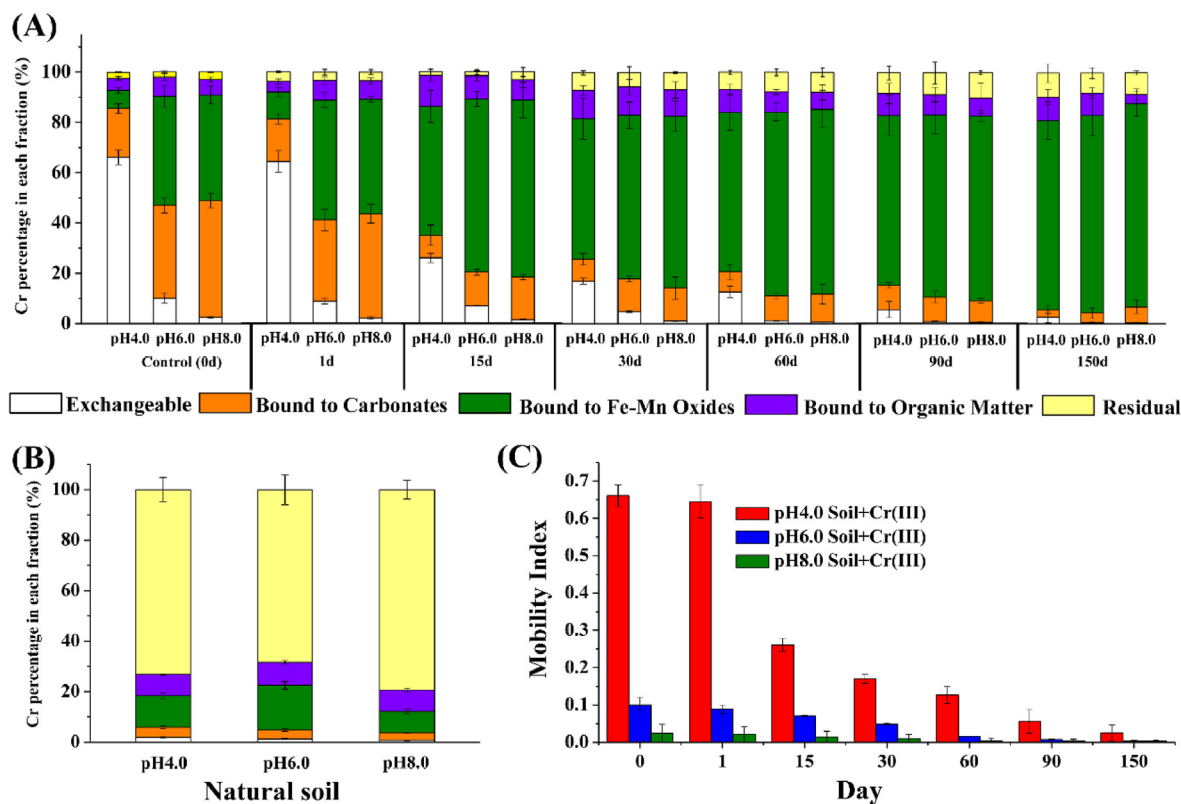


Fig. 2. (A) Effect of incubation time on the Cr fractionation (%) in three soil types after addition of Cr(III). The content of Cr in soils was 600 mg kg^{-1} . (B) The fractionation of Cr in natural soils with different pH levels (without addition of Cr(III)). The content of Cr in natural soil was 41 mg kg^{-1} . (C) Mobility index of Cr in various pH soils with addition of Cr(III) as influenced by incubation time.

Table 2

Parameters of diffusion model and reaction kinetics-based model.

Soil pH	Diffusion equation			Elovich equation		First-order equation		Second-order equation		
	A	B	R ²	$\alpha \times 10^{-2}$	β	R ²	k ₁	R ²	k ₂ × 10 ⁻⁴	R ²
pH4.0	5.58	-0.021	0.9427	-40.13	-0.015	0.9973	0.021	0.9427	4.5	0.9252
pH6.0	3.91	-0.023	0.9645	-3.81	-0.10	0.8000	0.023	0.9645	30.7	0.9245
pH8.0	2.34	-0.014	0.9254	-0.46	-0.50	0.9384	0.014	0.9254	34.7	0.9967

where Eh (mV) is the electrode potential, E⁰ (mV) is the standard potential, n is the number of electrons exchanged in the reaction, m is the number of protons exchanged, and parentheses include the activities of the oxidized and reduced species. Qualitatively analysis indicated that Eh increased with decreasing pH. However, Eh did not vary linearly with pH. Thus, m/n in the above equation was not constant in the soil. This inconsistency could be ascribed to complex soil components, such as silicates and oxides. In accordance with the Eh-pH diagram (Kaur and Crimi, 2014), Cr(VI)/Cr(III) couple favours Cr(VI) stabilization in soil with pH 8.0. In contrast, Cr(VI)/Cr(III) couple favours Cr(III) stabilization in soils with pH 6.0 and 4.0.

The first-order equation was used to fit Cr(III) oxidation data in pH 8.0 soil (Fig. 3C). The high correlation coefficient R² (0.9891) indicated that the oxidation process was of the first order, and the apparent rate constant was $1.04 \times 10^{-4} \text{ day}^{-1}$. The time required for half of Cr(III) to be converted into Cr(VI) was 6357 days based on the half-time ($t_{1/2}$) of $(\ln 2)/k_1$ for the reaction. Oxidation of Cr(III) to toxic Cr(VI) by MnO₂ has been identified as probably the important oxidation pathway in soils (Hausladen and Fendorf, 2017). In pH 8.0 soil, the active oxidizing sites on MnO₂ may be partly covered by the precipitation Cr(OH)₃ which limited the oxidation process and led to the low oxidation ratio of Cr(III) (Milacic and Stupar, 1995). However, the quantity of Cr(VI)

was dependent on the initial concentration of Cr(III) released into soils according to the kinetic analysis. These findings may help to understand the serious environmental risks associated with alkaline soils contaminated by Cr(III) for a long time due to the continuous conversion of Cr(III) into hazardous Cr(VI).

3.5. Spectral characterization of soils amended with Cr(III) at three pH levels

Soil with preadjusted pH (pH 4.0, 6.0, and 8.0) were amended with Cr(III) (600 mg kg^{-1}) and incubated for 90 days at 303 K before FTIR analysis. Fig. 4(A-C) displays the comparison of the FTIR spectra of soils before and after amendment with Cr(III). Before the application of Cr(III), a broad intense band appeared near 3437 cm^{-1} , which could be a characteristic of hydroxy (Ramrakhiani et al., 2011). The bands then shifted to 3415 cm^{-1} after the acidification of soil due to the formation of new H-bonded hydroxyl groups. The band around 1430 cm^{-1} represented carbonate in the spectra of pH 8.0 soil (Ghorbel-Abid et al., 2009). Meanwhile, the peak disappeared for pH 4.0 and 6.0 soils due to the decomposition of carbonate, resulting in the lower proportion of CB Cr in acid soil than in alkaline soil (Fig. 2A). The decomposition of carbonate was also related to the decrease of the content of soil

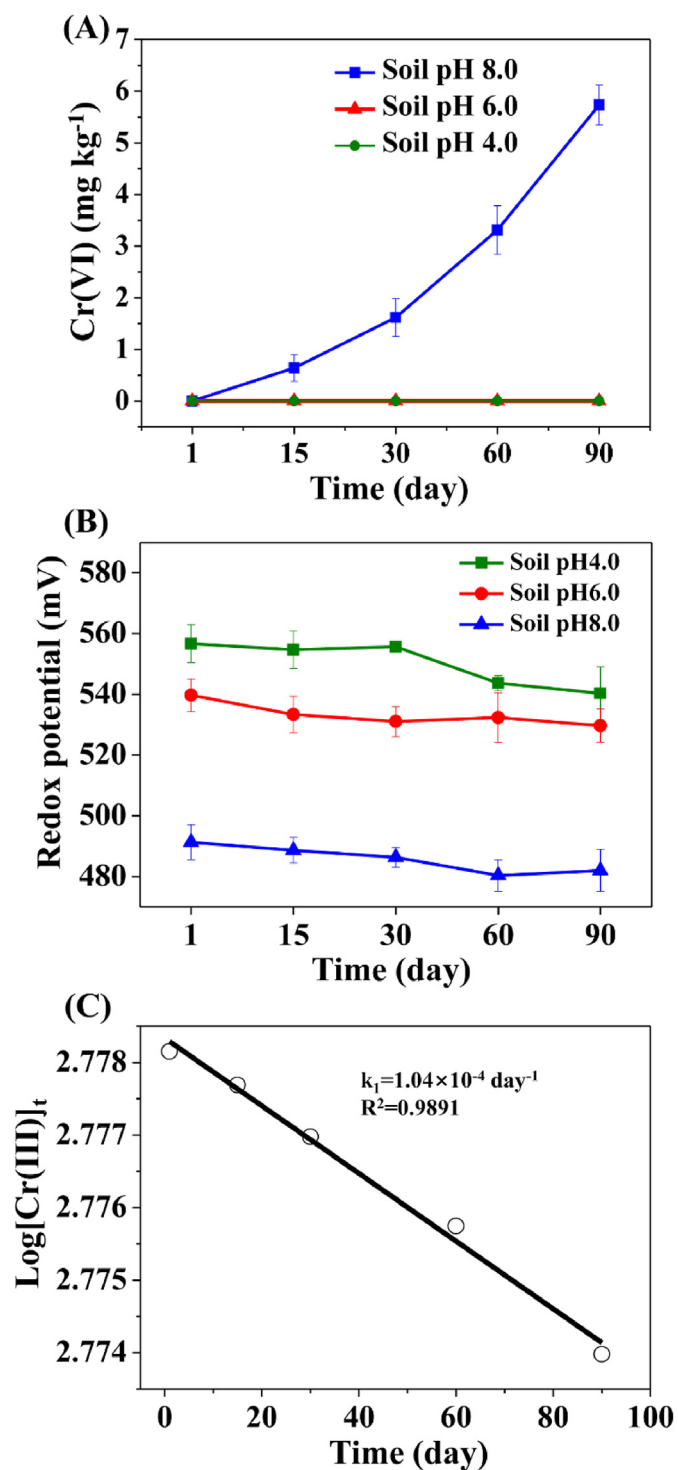


Fig. 3. (A) Kinetic of formation of Cr(VI) in three types of soil, (B) redox potential in soils with Cr(III) treatment as a function of incubation time at three pH levels, (C) first-order kinetic model fitting of Cr(III) oxidation kinetics data in pH 8.0 soil. Error bars represented the results of three measurements. The initial concentration of Cr(III) in the soil was 600 mg kg⁻¹ and without Cr(VI).

inorganic carbon (Table 1). The peaks around 1032 cm⁻¹ in the three spectra represented the stretching vibration of Si-O and C-O (Li et al., 2011; Zhang et al., 2018a). The bands for soils with pH 4.0 and 6.0 appeared a new peak and centered at 1140 cm⁻¹ and 1141 cm⁻¹, respectively, possibly because the quartz was really had to be broken and some phyllosilicates were changed due to the soil acidification. The results showed that soil pH resulted in variations in soil compositions

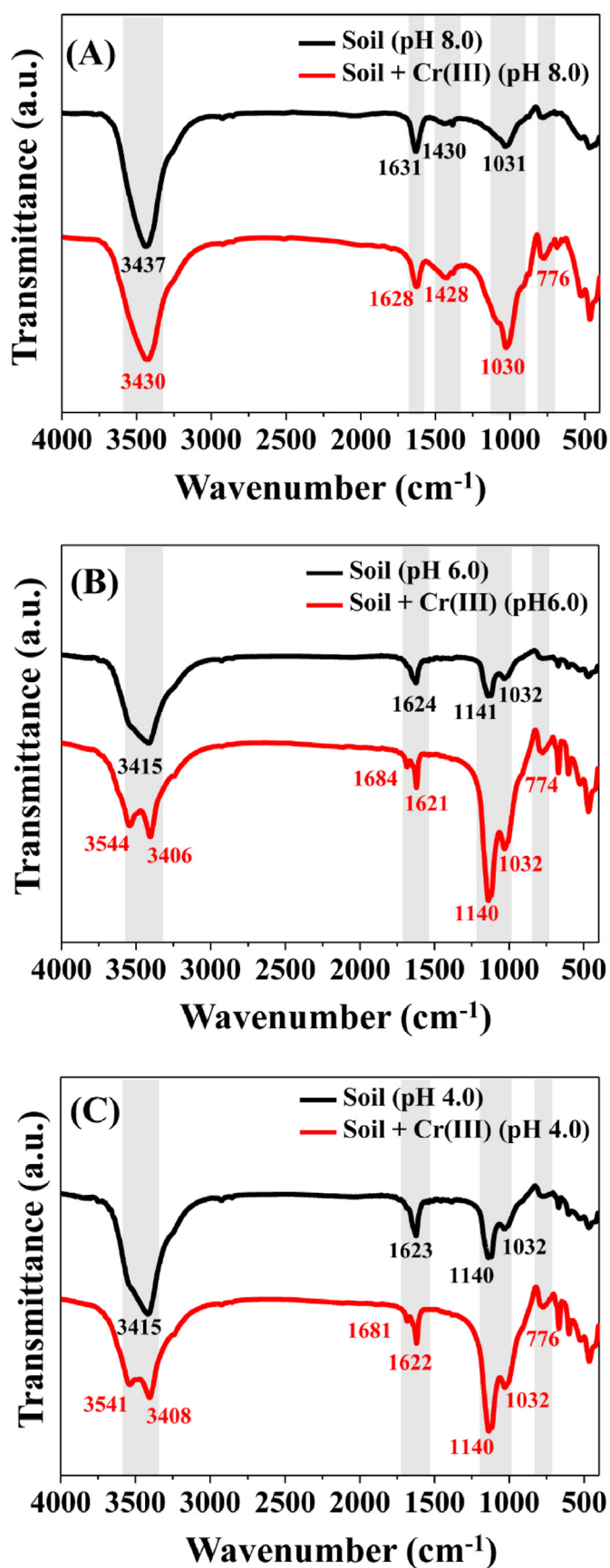


Fig. 4. FT-IR spectra of (A) pH 8.0 soil before and after Cr(III) treatment, (B) pH 6.0 soil before and after Cr(III) treatment, (C) pH 4.0 soil before and after Cr(III) treatment. The initial content of Cr(III) in the soil were 600 mg kg⁻¹ and the incubation time were 90 days.

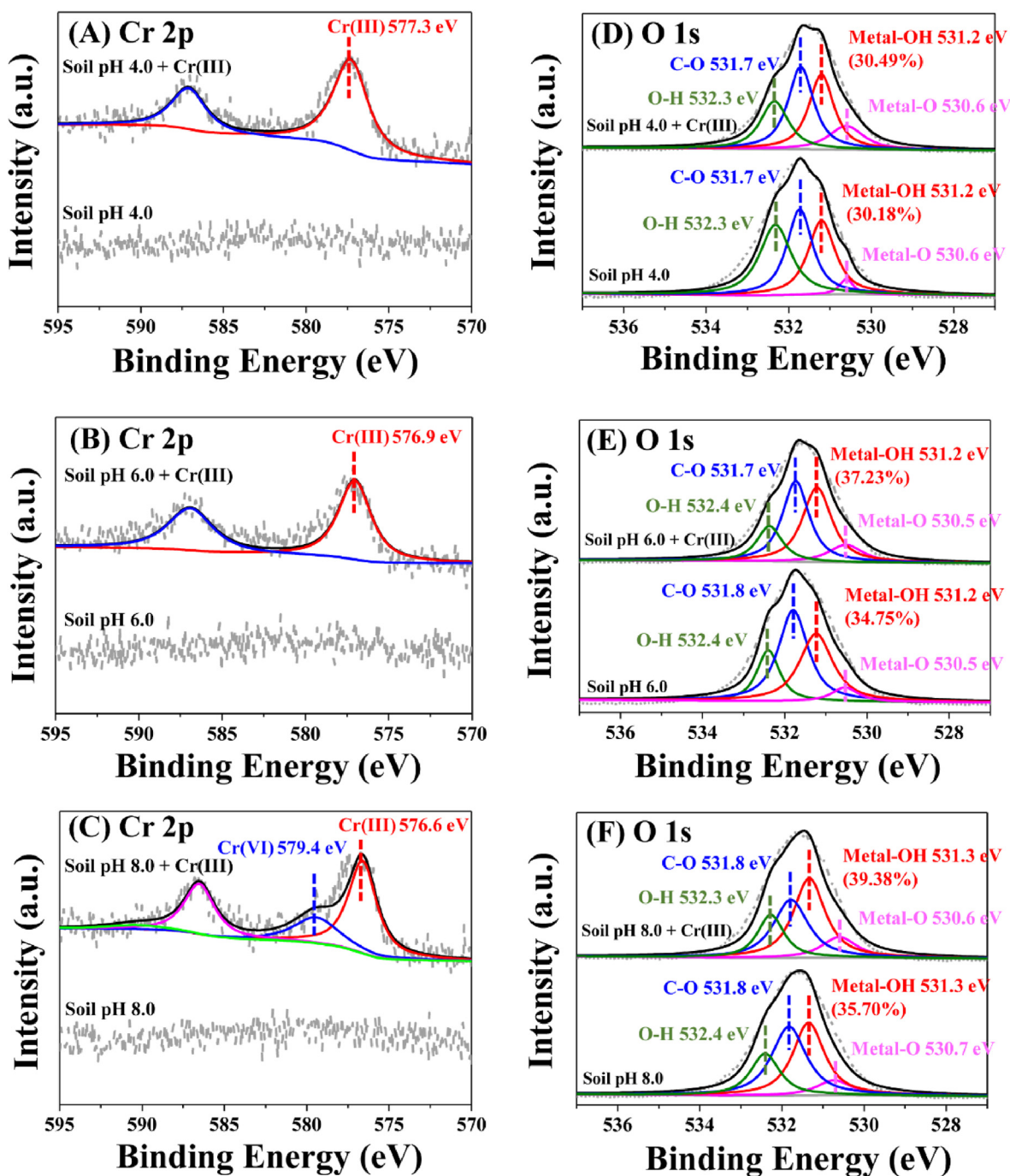


Fig. 5. The Cr 2p XPS spectra of soils with or without addition of Cr(III) at (A) pH 4.0, (B) pH 6.0, and (C) pH 8.0. The O 1s XPS spectra of soils with or without addition of Cr(III) at (D) pH 4.0, (E) pH 6.0, and (F) pH 8.0. The initial content of Cr(III) in soils were 5000 mg kg⁻¹ and the incubation time were 90 days.

and mineralogical properties, thereby altering soil surface properties, such as CEC and charge.

After the application of Cr(III), the bands at 3415 cm⁻¹ split into two peaks around 3544 cm⁻¹ and 3406 cm⁻¹ for soils with pH 4.0 and 6.0, indicating the interaction of Cr(III) with the hydroxyl of soils, such as silanol or carboxyl. In the meantime, a new peak appeared at 1681 cm⁻¹ for pH 4.0 soil and 1684 cm⁻¹ for pH 6.0 soil respectively, signifying the chelation of carboxyl with Cr(III) (Fathima et al., 2012), which is very different from that of soil with pH 8.0. Whereas the intensity of peaks at 774 to 776 cm⁻¹ slightly increased in all soils due to Cr–O vibration (Mishra et al., 2012), indicating the binding of the functional groups in soils with Cr(III). The different combinations of anthropogenic Cr(III) with functional groups in soils may affect Cr(III)

fractionation and retention. In addition, the peak intensity at 1140 cm⁻¹ or 1032 cm⁻¹ representing the stretching bands of Si–O increased obviously after the amendment of Cr(III), just as the finding of Fathima et al. (2012). This may be ascribed to the initial Cr(III) solution with low pH (about 4.0) resulting in phyllosilicates changed.

Soils with preadjusted pH were amended with 5000 mg kg⁻¹ Cr(III) and incubated for 90 days prior to XPS analyses. The wide-scan XPS spectra of soils before and after amended with Cr(III) at three pH levels were displayed in supplementary date (Fig. S5). Fig. 5A–C shows the comparison of Cr 2p XPS spectra of soils with or without addition of Cr(III) at three pH levels. Before adding Cr(III) to the soil, there were no obvious Cr peak in the spectrum due to the low Cr content in the natural soil. The Cr 2p peaks clearly appeared in the spectrum of soils after

addition of Cr(III). The $2p_{3/2}$ lines were located at 577.3, 576.9 and 576.6 eV for soils with pH of 4.0–8.0, respectively. These lines were characteristic of Cr(III), and the binding energy decreased with soil pH. According to literature (Jung et al., 2007), the Cr $2p_{3/2}$ binding energies of chromic hydroxides were within 576.5–576.9 eV. Then $2p_{3/2}$ peaks indicated chromic hydroxides as dominant species in pH 8.0 soil rather than in pH 4.0 soil, verifying the precipitate retention mechanism of Cr(III) in alkaline soil suggested in batch sorption experiments. Furthermore, the binding energy of the $2p_{3/2}$ signal was centered at 579.4 eV for pH 8.0 soil, which was characteristic of Cr(VI) (Boursiquot et al., 2002). This was consistent with the presence of Cr(VI) in incubation experiments (section 3.4). No evident shoulder was found near 579 eV for soils with pH 4.0 and 6.0. Accordingly, the use of a component attributable to Cr(VI) did not achieve a satisfactory fit. The concentration-enhanced incubation samples further confirmed that Cr(III) in alkaline soils was converted into Cr(VI) in contrast to that in acidic soils. This result was consistent with the oxidation kinetics experiment.

Fig. 5D–F displays the O 1s spectra of soils with various pH levels before and after amended with Cr(III). The O 1s spectra could be resolved into four peaks. Before adding Cr(III) to soils, the binding energies of the signals were located at 530.7, 531.3, 531.8, and 532.4 eV in pH 8.0 soil, representing metal-oxide, metal-hydroxide (e.g., Fe–OH), C–O, and O–H bonds, respectively (Lyu et al., 2018). As illustrated in Fig. 5D–F, an obvious increase of the relative peak area associated with metal-OH bonds could be found in soils with pH 8.0 (about 3.68%) after the addition of Cr(III), indicating the formation of Cr–OH and corroborating chromic hydroxide as dominate species in alkaline soil showing in Cr $2p_{3/2}$ spectra. In pH 4.0 soil, the relative peak area at 531.2 eV increased little (about 0.31%) after the addition of Cr(III), indicating that no chromic hydroxide was formed and also corroborating the Cr $2p_{3/2}$ spectra of pH 4.0 soil.

4. Conclusions

This study aimed to investigate the effect of soil pH on the transport, fractionation, and oxidation behavior of Cr(III). The soil column study showed that the alkaline soil had the best ability to retard the transport of Cr(III) and the easy occurrence of transport of Cr(III) in the acidic soil. The batch sorption experiments revealed that the high retention of Cr(III) in pH 8.0 soil was mainly attributed to the precipitate. The limited chemisorption elucidated the low retention of Cr(III) in acidic soils. The FTIR spectra confirmed the interaction of Cr(III) with hydroxyl and carboxyl in soils with pH 4.0 and pH 6.0. XPS analysis confirmed the formation of higher amounts of chromic hydroxides in the alkaline soil than in the acidic soil. These findings may help us understand that Cr(III) was likely to expand the pollution range in acidic soils and further contaminate groundwater.

The fraction determination results indicated higher exchangeable Cr in the acidic soil than in the alkaline soil, especially at the early stage of incubation. This finding confirmed the easy mobility of Cr in acidic soils in cases where seepage of Cr(III) occurred. The exchangeable Cr would transform into other more stable species over time. At the end of 150 days incubation, the content of EX Cr fraction in the three types of soils was reduced to very low level. The time-dependent transformation well fitted by the diffusion- and reaction-kinetics models, thereby indicating the mass transfer of the exchangeable Cr through soil micropores and mesopores and as chemical transforming occurred simultaneously. This transformation study illustrated the high risk at the early stage of the anthropogenic Cr(III) entering the acidic soil because exchangeable Cr was considered high mobility and represented bioavailability for the ecosystem.

Hazardous Cr(VI) was spontaneously formed in pH 8.0 soil due to the appropriate Eh, confirmed by XPS spectra. The Cr(VI) content increased with incubation time, and the first-ordered kinetics equation could better described the oxidation rate, which was proportional to the first power of the initial Cr(III) concentration. Hence, the potential

environmental risks of Cr(III) in alkaline soil were related to the initial concentration of Cr(III) released and increased with incubation time. This work provides a basis for understanding the environmental impact of anthropogenic Cr(III) affected by soil pH.

CRedit authorship contribution statement

Teng Xu: Conceptualization, Methodology, Writing - original draft. **Feng Nan:** Investigation, Resources. **Xiaofeng Jiang:** Formal analysis. **Yuling Tang:** Software. **Yunhang Zeng:** Writing - review & editing. **Wenhua Zhang:** Writing - review & editing, Supervision. **Bi Shi:** Supervision.

Declaration of competing interests

The authors declare that they have no known competing financial interests or personal relationships that could have appeared to influence the work reported in this paper.

Acknowledgement

This work was funded by the National Key Research and Development Program of China (No. 2018YFC1802201).

Appendix A. Supplementary data

Supplementary data to this article can be found online at <https://doi.org/10.1016/j.ecoenv.2020.110459>.

References

- Aceves, M.B., Hernandez, J.C., Vazquez, R.R., 2007. Chromium fractionation in semi-arid soils amended with chromium and tannery sludge. *J. Hazard Mater.* 146 (1–2), 91–97. <https://doi.org/10.1016/j.jhazmat.2006.12.001>.
- Akhtar, M.S., Stüben, D., Norra, S., Memon, M., 2011. Soil structure and flow rate-controlled molybdate, arsenate and chromium (III) transport through field columns. *Geoderma* 161 (3–4), 126–137. <https://doi.org/10.1016/j.geoderma.2010.12.005>.
- Ali, Z., Malik, R.N., Shinwari, Z.K., Qadir, A., 2015. Enrichment, risk assessment, and statistical apportionment of heavy metals in tannery-affected areas. *Int. J. Environ. Sci. Technol.* 12 (2), 537–550. <https://doi.org/10.1007/s13762-013-0428-4>.
- Alibardi, L., Cossu, R., 2016. Pre-treatment of tannery sludge for sustainable landfilling. *Waste Manag.* 52, 202–211. <https://doi.org/10.1016/j.wasman.2016.04.008>.
- Balasoju, C.F., Zagury, G.J., Deschenes, L., 2001. Partitioning and speciation of chromium, copper, and arsenic in CCA-contaminated soils: influence of soil composition. *Sci. Total Environ.* 280 (1–3), 239–255. [https://doi.org/10.1016/S0048-9697\(01\)00833-6](https://doi.org/10.1016/S0048-9697(01)00833-6).
- Banks, M.K., Schwab, A.P., Henderson, C., 2006. Leaching and reduction of chromium in soil as affected by soil organic content and plants. *Chemosphere* 62 (2), 255–264. <https://doi.org/10.1016/j.chemosphere.2005.05.020>.
- Bartlett, R., James, B., 1979. Behavior of chromium in soils: III. Oxidation I. *J. Environ. Qual.* 8 (1), 31–35. <https://doi.org/10.2134/jeq1979.00472425000800010008x>.
- Boursiquot, S., Mullet, M., Ehrhardt, J.J., 2002. XPS study of the reaction of chromium (VI) with mackinawite (FeS). *Surf. Interface Anal.* 34 (1), 293–297. <https://doi.org/10.1002/sia.1303>.
- Brady, J.E., Humiston, G.E., Heikkinen, H., 1990. *General Chemistry: Principles and Structure*. Wiley, pp. 288.
- Calderer, M., Martí, V., De-Pablo, J., Guivernau, M., Prenafeta-Boldu, F.X., Vinas, M., 2014. Effects of enhanced denitrification on hydrodynamics and microbial community structure in a soil column system. *Chemosphere* 111, 112–119. <https://doi.org/10.1016/j.chemosphere.2014.03.033>.
- Castillo, A.N., García-Delgado, R.A., Rivero, V.C., 2012. Electrokinetic treatment of soils contaminated by tannery waste. *Electrochim. Acta* 86 (30), 110–114. <https://doi.org/10.1016/j.electacta.2012.04.132>.
- Choppala, G., Kunhikrishnan, A., Seshadri, B., Park, J.H., Bush, R., Bolan, N., 2018. Comparative sorption of chromium species as influenced by pH, surface charge and organic matter content in contaminated soils. *J. Geochem. Explor.* 184, 255–260. <https://doi.org/10.1016/j.gexplo.2016.07.012>.
- Covington, A.D., 2009. *Tanning Chemistry: the Science of Leather*. Royal Society of Chemistry, pp. 185.
- Dean, J.A., 1999. In: Esposito, R. (Ed.), *Lange's Handbook of Chemistry*. McGraw-Hill, pp. 8–9.
- Ertani, A., Mietto, A., Borin, M., Nardi, S., 2017. Chromium in agricultural soils and crops: a review. *Water, Air, Soil Poll.* 228, 190. <https://doi.org/10.1007/s11270-017-3356-y>.
- Farid, M., Ali, S., Rizwan, M., Ali, Q., Saeed, R., Nasir, T., Abbasi, G.H., Rehmani, M.I.A., Ata-Ul-Karim, S.T., Bukhari, S.A.H., Ahmad, T., 2018. Phyto-management of

- chromium contaminated soils through sunflower under exogenously applied 5-amino-nolevulinic acid. *Ecotoxicol. Environ. Saf.* 151, 255–265. <https://doi.org/10.1016/j.ecoenv.2018.01.017>.
- Fathima, A., Rao, J.R., Nair, B.U., 2012. Trivalent chromium removal from tannery effluent using kaolin-supported bacterial biofilm of *Bacillus* sp isolated from chromium polluted soil. *J. Chem. Technol. Biotechnol.* 87 (2), 271–279. <https://doi.org/10.1002/jctb.2710>.
- Flogeac, K., Guillon, E., Aplincourt, M., 2005. Adsorption of several metal ions onto a model soil sample: equilibrium and EPR studies. *J. Colloid Interface Sci.* 286 (2), 596–601. <https://doi.org/10.1016/j.jcis.2005.01.027>.
- Font, R., Gomis, V., Fernandez, J., Sabater, M.C., 1998. Physico-chemical characterization and leaching of tannery wastes. *Waste Manag. Res.* 16 (2), 139–149. <https://doi.org/10.1177/0734242X9801600206>.
- Fu, R., Wen, D., Xia, X., Zhang, W., Gu, Y., 2017. Electrokinetic remediation of chromium (Cr)-contaminated soil with citric acid (CA) and polyaspartic acid (PASP) as electrolytes. *Chem. Eng. J.* 316 (15), 601–608. <https://doi.org/10.1016/j.cej.2017.01.092>.
- Ghorbel-Abid, I., Jrad, A., Nahdi, K., Trabelsi-Ayadi, M., 2009. Sorption of chromium (III) from aqueous solution using bentonitic clay. *Desalination* 246 (1–3), 595–604. <https://doi.org/10.1016/j.desal.2008.05.029>.
- Godoy, V.A., Zuquette, L.V., Gómez-Hernández, J.J., 2019. Stochastic upscaling of hydrodynamic dispersion and retardation factor in a physically and chemically heterogeneous tropical soil. *Stoch. Environ. Res. Risk Assess.* 33 (1), 201–216. <https://doi.org/10.1007/s00477-018-1624-z>.
- Gustafsson, J.P., Persson, I., Oromieh, A.G., van-Schaik, J.W.J., Sjøstedt, C., Kleja, D.B., 2014. Chromium (III) complexation to natural organic matter: mechanisms and modeling. *Environ. Sci. Technol.* 48 (3), 1753–1761. <https://doi.org/10.1021/es404557e>.
- Hausladen, D.M., Fendorf, S., 2017. Hexavalent chromium generation within naturally structured soils and sediments. *Environ. Sci. Technol.* 51 (4), 2058–2067. <https://doi.org/10.1021/acs.est.6b04039>.
- Hu, L., Diez-Rivas, C., Hasan, A.R., Solo-Gabriele, H., Fieber, L., Cai, Y., 2010. Transport and interaction of arsenic, chromium, and copper associated with CCA-treated wood in columns of sand and sand amended with peat. *Chemosphere* 78 (8), 989–995. <https://doi.org/10.1016/j.chemosphere.2009.12.019>.
- Jardine, P.M., Fendorf, S.E., Mayes, M.A., Larsen, I.L., Brooks, S.C., Bailey, W.B., 1999. Fate and transport of hexavalent chromium in undisturbed heterogeneous soil. *Environ. Sci. Technol.* 33 (17), 2939–2944. <https://doi.org/10.1021/es981211v>.
- Jung, Y., Choi, J., Lee, W., 2007. Spectroscopic investigation of magnetite surface for the reduction of hexavalent chromium. *Chemosphere* 68 (10), 1968–1975. <https://doi.org/10.1016/j.chemosphere.2007.02.028>.
- Kantar, C., Demiray, H., Dogan, N.M., 2011. Role of microbial exopolymeric substances (EPS) on chromium sorption and transport in heterogeneous subsurface soils: II. Binding of Cr (III) in EPS/soil system. *Chemosphere* 82 (10), 1496–1505. <https://doi.org/10.1016/j.chemosphere.2010.11.001>.
- Kaur, K., Crimi, M., 2014. Release of chromium from soils with persulfate chemical oxidation. *Groundwater* 52 (5), 748–755. <https://doi.org/10.1111/gwat.12116>.
- Li, G., Yang, X., Liang, L., Guo, S., 2017. Evaluation of the potential redistribution of chromium fractionation in contaminated soil by citric acid/sodium citrate washing. *Arab. J. Chem.* 10 (S1), S539–S545. <https://doi.org/10.1016/j.arabjc.2012.10.016>.
- Li, Y., Li, T., Jin, Z., 2011. Stabilization of Fe⁰ nanoparticles with silica fume for enhanced transport and remediation of hexavalent chromium in water and soil. *J. Environ. Sci.* 23 (7), 1211–1218. [https://doi.org/10.1016/S1001-0742\(10\)60534-7](https://doi.org/10.1016/S1001-0742(10)60534-7).
- Löv, A., Sjøstedt, C., Larsbo, M., Persson, I., Gustafsson, J.P., Cornelis, G., Kleja, D.B., 2017. Solubility and transport of Cr (III) in a historically contaminated soil—evidence of a rapidly reacting dimeric Cr (III) organic matter complex. *Chemosphere* 189, 709–716. <https://doi.org/10.1016/j.chemosphere.2017.09.088>.
- Lu, A., Zhang, S., Shan, X., 2005. Time effect on the fractionation of heavy metals in soils. *Geoderma* 125 (3–4), 225–234. <https://doi.org/10.1016/j.geoderma.2004.08.002>.
- Lyu, H., Zhao, H., Tang, J., Gong, Y., Huang, Y., Wu, Q., Gao, B., 2018. Immobilization of hexavalent chromium in contaminated soils using biochar supported nanoscale iron sulfide composite. *Chemosphere* 194, 360–369. <https://doi.org/10.1016/j.chemosphere.2017.11.182>.
- Makdissi, R.S., 1991. Tannery wastes definition, risk assessment and cleanup options, Berkeley, California. *J. Hazard Mater.* 29 (1), 79–96. [https://doi.org/10.1016/0304-3894\(91\)87075-D](https://doi.org/10.1016/0304-3894(91)87075-D).
- Milacic, R., Stupar, J., 1995. Fractionation and oxidation of chromium in tannery waste- and sewage sludge-amended soils. *Environ. Sci. Technol.* 29 (2), 506–514. <https://doi.org/10.1021/es00002a029>.
- Mishra, R.R., Dhal, B., Dutta, S.K., Dangar, T.K., Das, N.N., Thatoi, H.N., 2012. Optimization and characterization of chromium (VI) reduction in saline condition by moderately halophilic *Vigribacillus* sp. isolated from mangrove soil of Bhitarkanika, India. *J. Hazard Mater.* 227–228 (15), 219–226. <https://doi.org/10.1016/j.jhazmat.2012.05.063>.
- Obia, A., Cornelissen, G., Mulder, J., Dorsch, P., 2015. Effect of soil pH increase by biochar on NO, N₂O and N₂ production during denitrification in acid soils. *PLoS One* 10 (9), e0138781. <https://doi.org/10.1371/journal.pone.0138781>.
- Panda, R.C., Selvasekar, S., Murugan, D., Sivakumar, V., Narayani, T., Sreepadha, C., 2016. Cleaner production of basic chromium sulfate—with a review of sustainable green production options. *J. Clean. Prod.* 112 (Part 5, 20), 4854–4862. <https://doi.org/10.1016/j.jclepro.2015.05.123>.
- Ramrakhiani, L., Majumder, R., Khowala, S., 2011. Removal of hexavalent chromium by heat inactivated fungal biomass of *Termitomyces clypeatus*: surface characterization and mechanism of biosorption. *Chem. Eng. J.* 171 (3), 1060–1068. <https://doi.org/10.1016/j.cej.2011.05.002>.
- Reijonen, I., Hartikainen, H., 2016. Oxidation mechanisms and chemical bioavailability of chromium in agricultural soil—pH as the master variable. *Appl. Geochem.* 74, 84–93. <https://doi.org/10.1016/j.apgeochem.2016.08.017>.
- Religa, P., Kowalik, A., Gierycz, P., 2011. Application of nanofiltration for chromium concentration in the tannery wastewater. *J. Hazard Mater.* 186 (1), 288–292. <https://doi.org/10.1016/j.jhazmat.2010.10.112>.
- Shahid, M., Shamsad, S., Rafiq, M., Khalid, S., Bibi, I., Niazi, N.K., Dumat, C., Rashid, M.I., 2017. Chromium speciation, bioavailability, uptake, toxicity and detoxification in soil-plant system: a review. *Chemosphere* 178, 513–533. <https://doi.org/10.1016/j.chemosphere.2017.03.074>.
- Sparks, D.L., 2003. In: Crumly, C.R. (Ed.), *Environmental Soil Chemistry*. Elsevier, pp. 214–215.
- Su, H., Fang, Z., Tsang, P.E., Zheng, L., Cheng, W., Fang, J., Zhao, D., 2016. Remediation of hexavalent chromium contaminated soil by biochar-supported zero-valent iron nanoparticles. *J. Hazard Mater.* 318 (15), 533–540. <https://doi.org/10.1016/j.jhazmat.2016.07.039>.
- Sun, X., Huang, X., Liao, X., Shi, B., 2011. Adsorptive removal of Cu (II) from aqueous solutions using collagen-tannin resin. *J. Hazard Mater.* 186 (2–3), 1058–1063. <https://doi.org/10.1016/j.jhazmat.2010.11.098>.
- Taghipour, M., Jalali, M., 2015. Effect of clay minerals and nanoparticles on chromium fractionation in soil contaminated with leather factory waste. *J. Hazard Mater.* 297 (30), 127–133. <https://doi.org/10.1016/j.jhazmat.2015.04.067>.
- Tessier, A., Campbell, P.G.C., Bisson, M., 1979. Sequential extraction procedure for the speciation of particulate trace metals. *Anal. Chem.* 51 (7), 844–851. <https://doi.org/10.1021/ac50043a017>.
- Zhang, C., Xia, F., Long, J., Peng, B., 2017. An integrated technology to minimize the pollution of chromium in wet-end process of leather manufacture. *J. Clean. Prod.* 154 (15), 276–283. <https://doi.org/10.1016/j.jclepro.2017.03.216>.
- Zhang, J., Yin, H., Wang, H., Xu, L., Samuel, B., Liu, F., Chen, H., 2018a. Reduction mechanism of hexavalent chromium by functional groups of undissolved humic acid and humin fractions of typical black soil from Northeast China. *Environ. Sci. Pollut. Res.* 25 (17), 16913–16921. <https://doi.org/10.1007/s11356-018-1878-5>.
- Zhang, X., Tong, J., Hu, B., Wei, W., 2018b. Adsorption and desorption for dynamics transport of hexavalent chromium (Cr (VI)) in soil column. *Environ. Sci. Pollut. Res.* 25 (1), 459–468. <https://doi.org/10.1007/s11356-017-0263-0>.
- Zhou, J., Hu, S., Wang, Y., He, Q., Liao, X., Zhang, W., Shi, B., 2012. Release of chrome in chrome tanning and post tanning processes. *J. Soc. Leather Technol. Chem.* 96 (4), 157–162.
- Zhou, W., Long, W., Xu, T., Peng, L., Zhang, W., 2019. Organic ligands unexpectedly increase the toxicity of chromium (III) for luminescent bacteria. *Environ. Chem. Lett.* 17 (4), 1849–1855. <https://doi.org/10.1007/s10311-019-00892-y>.